17

Materials and techniques for energy harvesting

M. E. KIZIROGLOU and E. M. YEATMAN,
Imperial College London, UK

Abstract: Energy harvesting, the collection of small amounts of ambient energy to power wireless devices, is a very promising technology for applications where batteries are impractical, such as body sensor networks and inaccessible remote systems. The performance and potential of energy-harvesting devices depend strongly on the performance and specific properties of materials. In this chapter the important properties and potential of materials used in energy-harvesting devices are reviewed. An introduction to the concept of energy harvesting is given with a special discussion on motion energy-harvesting limits. The state of the art of materials for piezoelectric, electrostatic, thermoelectric and electromagnetic harvesting devices is discussed, with emphasis on desired material properties and corresponding available materials. In addition to the materials required in the energy transduction mechanism itself, the performance of mechanical oscillators at small scales is a critical factor in motion energy harvesting. For this reason, material requirements, performance and limitations for the implementation of low-frequency and broadband mechanical oscillators are reviewed in the final section of this chapter.

Key words: energy harvesting, MEMS, generator, piezoelectric, electrostatic, thermoelectric.

17.1 Introduction

Energy harvesting is one of the key emerging technologies of the twenty-first century. It refers to the collection of energy from the environment; energy that would otherwise be lost to heat. In order to distinguish from renewable energy sources more generally, energy harvesting can be defined as the collection of local naturally available energy for local use. Most often it involves small systems with tiny amounts of power, in the range from nanowatts to hundreds of milliwatts.

The main category of applications at these power levels is wireless devices. The applicability of energy harvesting to particular devices depends on the type and amount of the available ambient energy as well as on size limitations. It has been shown, for example, that energy harvesting from human motion

© Woodhead Publishing Limited, 2012

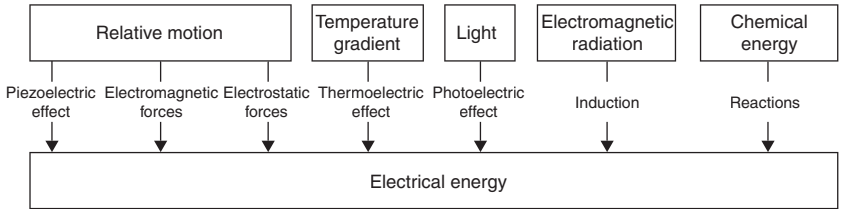

17.1 Categories of energy harvesting.

is generally not enough to power laptops or mobile phones, but is viable for many types of wireless sensors. Another important factor which has to be regarded when considering energy harvesting as a solution is whether batteries, the currently dominant wireless power source, are able to satisfy the power, size, weight, lifetime and ecological demands of the specific application.

Motion, temperature gradients, light, electromagnetic radiation and chemical energy can all be used as sources for energy harvesting. For motion, three different transduction mechanisms are available, namely electromagnetic, electrostatic and piezoelectric transduction. Thermal harvesters use the thermoelectric effect (also known as the Seebeck effect) and light harvesters the photoelectric effect, while electromagnetic harvesters use induction. Chemical harvesters can employ a variety of chemical reactions on the surface of electrodes. This categorization of different energy harvesters is illustrated in Fig. 17.1.

In the next section a theoretical analysis of motion energy harvesters is presented. Section 17.3 is focused on piezoelectric energy harvesting, emphasizing the role and critical properties of the materials employed. Electrostatic and thermoelectric harvesters and their materials are discussed in Sections 17.4 and 17.5. Electromagnetic energy harvesting from motion is presented in Section 17.6. Finally, a review of the materials used in suspension structures for motion energy harvesting in general is presented in Section 17.7.

17.2 Theory of motion energy harvesting

Motion energy-harvesting devices typically use a proof mass which can move with respect to the device frame. Energy can be transduced either by applying an external force directly to the proof mass or to the frame. The two device types are illustrated in Fig. 17.2. Taking the device frame as reference for motion, in the first case the force accelerates the proof mass, producing work which can be transduced to electrical energy. In the second case the force accelerates the frame, so with respect to the frame, an inertial force appears on the proof mass. The work of this inertial force is used to transduce energy.

© Woodhead Publishing Limited, 2012

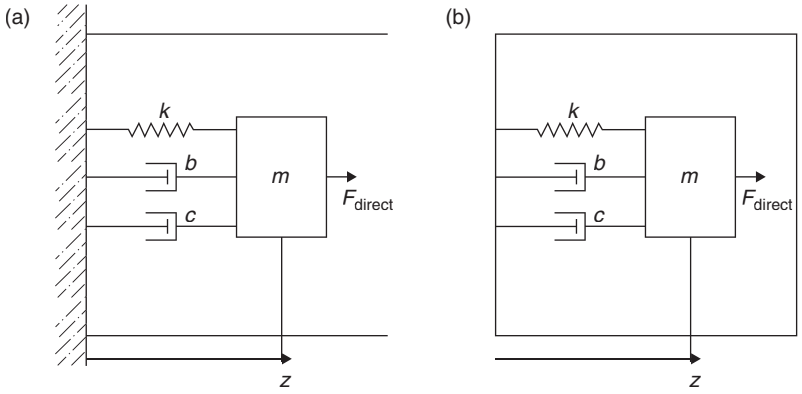

17.2 Typical model of a motion energy harvesting system. (a) Direct force harvester, (b) inertial force harvester.

Although direct force harvesting systems have been successfully implemented,[1] the inertial motion architecture is the most common. This is mainly because of the requirement of the direct force devices for physical contact with two objects in relative motion; the inertial devices require accelerating motion and only a single physical contact, which is usually more practical. Without loss of generality the following kinetic analysis will be performed on the inertial motion system of Fig. 17.2b. The proof mass m is bound to a frame through a mounting mechanism k. The mass can move relative to the frame either by application of direct force to it, or by application of a force on the frame. In both cases, the proof mass experiences a force F in relation to the frame. Due to k, the proof mass can move with respect to the frame and F can produce work, which is transduced into kinetic and potential energy (mechanism k, usually a type of strain) of the mass, but also to electrical energy through a mechanism b which acts as a force F_T. Parasitic damping can be modelled as a viscous mechanism c.

A general diagram of energy flow is given in Fig. 17.3. The part of F that is cancelled by F_T (does work against F_T) corresponds to direct transduction to electrical energy. The rest drives the motion of m, with the corresponding energy being exchanged between kinetic and potential forms. This stored energy can also be transduced to electrical through F_T (indirect transduction). During motion, the parasitic damping mechanism c is causing irreversible energy loss.

A general equation of motion for the system of Fig. 17.2 can be written as

$$F + F_T + F_k + F_d = m\ddot{z} \qquad [17.1]$$

where F, F_T, F_k and F_d are the external force (direct or inertial), the transduction force, the mounting mechanism force and the damping force

© Woodhead Publishing Limited, 2012

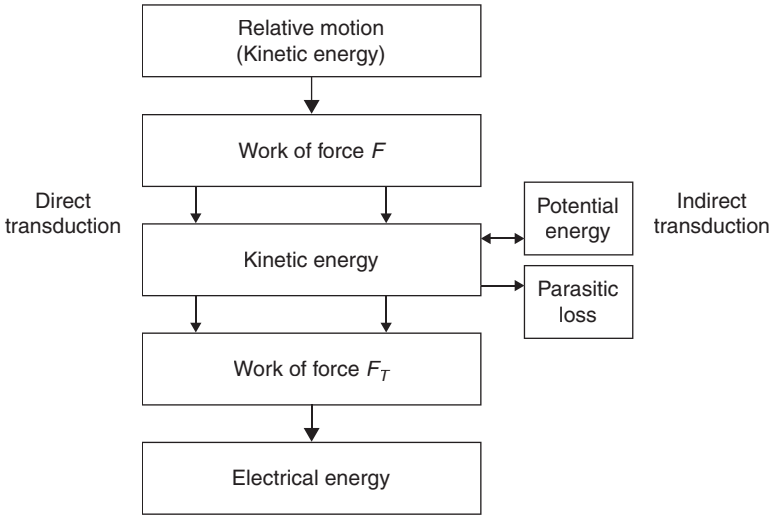

17.3 Direct and indirect energy transduction.

respectively, while $\ddot{z}$ is the acceleration of the proof mass m. The forces can be written as

$$\begin{aligned} F &= f_{dr}(t) \\ F_T &= f_T(z,\dot{z}) \\ F_k &= -f_k(z) \\ F_d &= -f_d(\dot{z}) \end{aligned} \qquad [17.2]$$

It is often the case in motion harvesting that the excitation can be approximated by a harmonic oscillation with angular frequency ω and amplitude Y_0, while the mounting mechanism is a linear spring system with a total spring constant k. Also, parasitic damping is usually mechanical friction. In this case Equations [17.2] can be written as

$$\begin{aligned} F &= F_0 \sin \omega t \\ F_T &= f_T(z,\dot{z}) \\ F_k &= -kz \\ F_d &= -c\dot{z} \end{aligned} \qquad [17.3]$$

The function $f_T(z,\dot{z})$ will depend on the transduction mechanism used. For reference, equations for some particular piezoelectric, electrostatic and

© Woodhead Publishing Limited, 2012

electromagnetic mechanisms are, respectively,

$$F_{\mathrm{T,pe}} = k_2 \cdot z + d \cdot A \cdot E$$
$$F_{\mathrm{T,es}} = \frac{1}{2} \cdot V^2 \frac{dC}{dz} \qquad [17.4]$$
$$F_{\mathrm{T,em}} = \frac{B^2 l^2 \dot{z}}{R}$$

In the first equation k_2 is the stiffness of the piezoelectric material, d is the direct piezoelectric effect coefficient, A is the area of application of $F_{T,\mathrm{pe}}$ and E is the corresponding electric field in the material. In the second equation, V is the voltage across a variable capacitor C consisting of two moving electrodes. Finally, in the third equation B is the magnetic flux density of a constant field, R is an ohmic electric load connected in parallel with a wire of length l moving perpendicularly to B and l with speed $\dot{z}$.

By assuming harmonic motion, an upper limit of the power for motion energy harvesters can be calculated as a function of device size (maximum internal displacement Z_l, mass m, vibration frequency ω and vibration amplitude Y_0):[2]

$$P_{\max} = \frac{2}{\pi} Y_0 Z_l \omega^3 m \qquad [17.5]$$

Using this equation, one can assess the viability of particular motion harvesting applications. In Fig. 17.4, the maximum power is plotted as a function

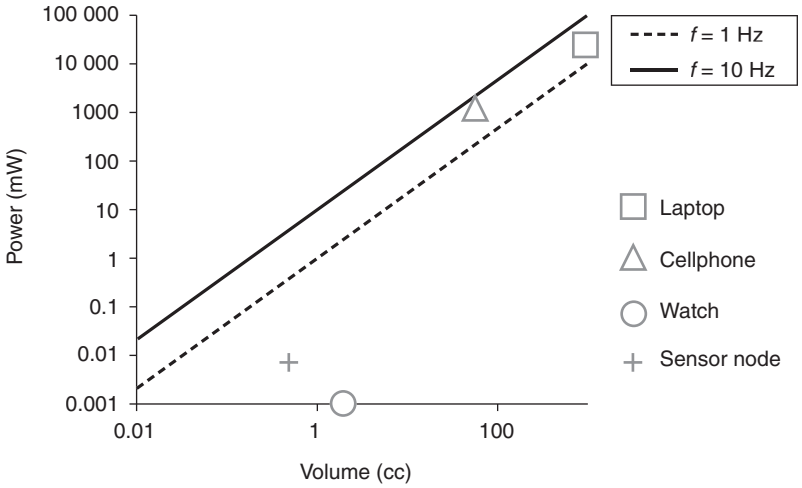

17.4 Maximum power for motion harvesters versus size for two different excitation frequencies, with size and power requirement of various applications superimposed.[2]

© Woodhead Publishing Limited, 2012

of device size for frequencies in the range expected for human motion, acceleration $\omega^2 Y_0$ of 10 m/s^2 and a proof mass density of 20 g/cm^3 occupying half of the device volume. By comparison with the power requirements and size of a typical laptop, cellphone, watch and sensor node, one concludes that human motion harvesting is not enough for the first two applications, while there is substantial promise for the last two. Indeed, the watch application has already been commercialized in high volumes, and sensors powered by harvesting are becoming more common.

17.3 Piezoelectric harvesting

In piezoelectric energy-harvesting devices, the piezoelectric effect is used to transform motion energy into electrical energy. Inertial motion of a proof mass results in mechanical stress in a piezoelectric material, which affects its electrical polarization, resulting in charge separation and thereby, in a voltage on the output. The ratio of generated polarization P over the applied mechanical stress σ in a piezoelectric material is called the piezoelectric coefficient:

$$d = \frac{P}{\sigma} \qquad [17.6]$$

One of the most popular piezoelectric materials is lead zirconate titanate (PZT). PZT is a ceramic perovskite consisting of lead zirconate and lead titanate. The phase diagram of the compound is shown in Fig. 17.5.[3] A morphotropic phase boundary (MPB) exists at a composition of 52% for lead

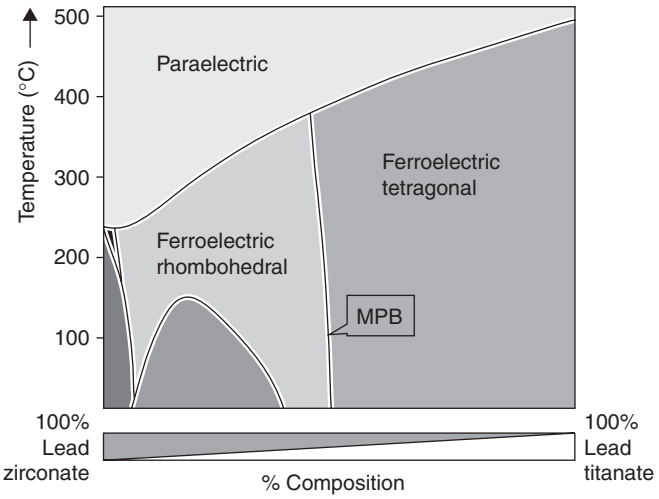

17.5 Phase diagram of lead zirconate–lead titanate compounds by Eric Cross.[3] (Source: Copyright 2004, Nature Publishing Group.)

© Woodhead Publishing Limited, 2012

zirconate, meaning that a large number of available domain states exists, for a wide temperature range. This property leads to a very high dielectric constant (ε_r = 1700), and high piezoelectric coefficients (e.g., d_{31} = –260 pC/N and k_{33} = 670 pC/N, for the NCE55 product of Micromechatronics Inc.[4]). Such attributes are very attractive for piezoelectric harvesting and this justifies the popularity of PZT in piezoelectric energy harvesting.

Apart from a high coupling coefficient which leads to high transduction efficiency, a critical material property for energy harvesting is its robustness. Most of the devices reported in the literature use stronger materials to form a thick beam which supports mechanically the piezoelectric layer. Metals such as aluminium, brass and steel and also silicon are used for this purpose.[5] The relative stiffness of the supporting beam with respect to that of the piezoelectric plays an important role on the overall efficiency of the structure. For example, aluminium has been shown to lead to higher efficiency compared to brass or steel.[6] The possibility of fabricating all-piezoelectric beams has been explored lately, employing thick film deposition and patterning techniques.[6] The achievement of thick enough, high-quality piezoelectric layers, giving reliable tolerance to high-acceleration peaks, is a key goal. The effect of the fabrication technique on the piezoelectric properties of the material is another important aspect. Maintenance of the properties of PZT even when the material is grown directly on the mechanical cantilever has been achieved, using techniques such as epitaxy[7] or sol-gel spin coating.[8]

PZT has been used in direct force motion-harvesting devices such as the 8.5 mW heel strike harvester which is based on a PZT bimorph structure.[1] PZT is also very common in inertial vibration energy-harvesting devices for low,[7,9] moderate[10] and high[11–13] vibration frequencies. A critical issue for such devices is that they require resonance operation to function efficiently and therefore their applicability is limited to vibration sources of particular, well-defined and stable frequencies. The resonance frequency of a typical cantilever structure is determined by its geometrical characteristics, and for micro-electro-mechanical systems (MEMS) devices, resonating at frequencies below 50 Hz is challenging. This is one of the main limiting factors in energy-harvesting applications.

An additional challenge for low-frequency vibration harvesting is that such sources usually have large vibration amplitudes which exceed the size of MEMS devices. Since there is no room for large proof mass vibration amplitude, a low Q is required. In such cases a material with high piezoelectric coefficient is critical, in order to achieve high enough damping with large electromechanical coupling.

Another well-known material which has been recently applied to energy-harvesting devices is lead magnesium niobate–lead titanate (PMN–PT).[14–16] The phase diagram of the compound is shown in Fig. 17.6. This material has been reported to result in energy harvesters with power at least an order of

© Woodhead Publishing Limited, 2012

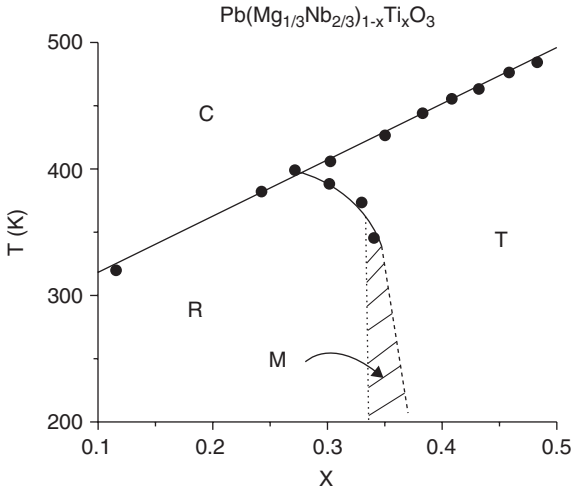

17.6 Phase diagram of lead magnesium niobate–lead titanate compounds from Ye *et al.*[16] (Source: Copyright 2001 by the American Physical Society.)

magnitude larger than PZT. This is due to the larger piezoelectric coefficient and stiffness of PMN–PT (e.g., $d_{11,\text{PZT-5H}} = 320$, $d_{31,\text{PMN-PT}} = 1063$ 9.1).[5] A comparison of the PZT and PMN–PT properties can be found in Reference 17. An important practical disadvantage of both PZT and PMN–PT materials is the existence of lead in their composition, which has been banned from use in commercial electronics.[18] For this reason, research on alternative materials to achieve highly piezoelectric properties without the use of toxic elements has been triggered. Results on alkaline niobate-based perovskite solid solutions indicate that these can have properties similar to PZT.[19]

Unlike piezoelectric sensors, where the required strain can be very low, piezoelectric energy harvesting requires as high a strain as possible and a large proof mass displacement in order to maximize energy transduction. This is very challenging for ceramic piezoelectrics as they are not tolerant to high strain. For this reason, more flexible materials are usually employed to form the cantilever while a thin piezoelectric layer is deposited near the supporting side.

The fragile nature of ceramic piezoelectrics in particular is a major limiting factor in maximizing vibration energy harvesting, especially for low-frequency–high-amplitude vibration sources. For this reason, piezoelectrics with high elasticity are particularly attractive. Such a piezoelectric material is polyvinylidene fluoride (PVDF). The monomer of PVDF chains ($-CH_2CF_2-$) exhibits a small polarization which, in aligned orientations can lead to macroscopic polarization and hence piezoelectricity, ferroelectricity and pyroelectricity. In α-phase PVDF, polarizations cancel each other, while in β-phase PVDF polarizations add together.[20] The β-phase polymeric

© Woodhead Publishing Limited, 2012

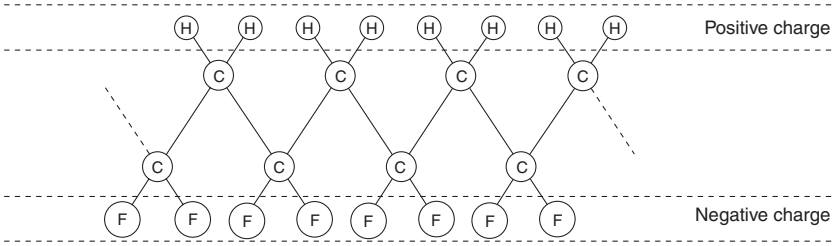

17.7 Polarization of a polymer chain in β-PVDF.

structure of PVDF is illustrated in Fig. 17.7. This alignment can be achieved by mechanical stretching and subsequent application of a large static electric field at elevated temperatures. This process is called poling. Further details can be found in Sencadas *et al.*[21]

PVDF has moderate piezoelectric coefficients (e.g., $d_{31} \approx 20$ pC/N and $d_{31} \approx 30$ pC/N for a uniaxial oriented PVDF film[20]) but very high elasticity which allows very high strain to be applied and large proof mass displacement. These features lead to large energy transduction, making PVDF a very attractive material for piezoelectric harvesting. PVDF has been used successfully in a backpack-mounted motion-harvesting device.[22] An elastic modulus of 5 GPa is reported, more than 10 times less than that of PZT, at 52 μm thickness, allowing a tenfold decrease in stress for a given strain. This feature allowed long device oscillation amplitude at low frequency, with harvested power output in the range of mW. A schematic of the device is shown in Fig. 17.8.

Furthermore, the demand for elastic piezoelectric materials in energy-harvesting applications has led to research on suitable composites that would combine high piezoelectric coefficients with high elasticity. A promising class of materials is macro-fibre composites (MFCs), which were initially developed for piezoelectric actuation applications.[8] Such materials are made by integration of piezoelectric fibres into a carrier material, in a particular orientation. A typical structure is described in Fig. 17.9. The carrier material is a polyimide film. The active layer consists of an array of parallel PZT fibres separated by epoxy. Apart from being piezoelectric, this layer also improves the strength of the elastic carrier. Conducting electrodes are also integrated into the MFC in the form of parallel Cu stripes again separated by epoxy, in a perpendicular orientation compared with the piezoelectric fibre array. In this way, the d_{33} piezoelectric coefficient is exploited, which is larger compared to the d_{31} typically used in monolithic PZT structures. MFCs have been applied as piezoelectric sensors for structural monitoring and in inflatable structures for space applications as alternatives to PVDF.[8,23]

Although the properties of MFCs are also promising for sensing and harvesting, the reported activity on such applications is limited to a few implementations.[24]

© Woodhead Publishing Limited, 2012

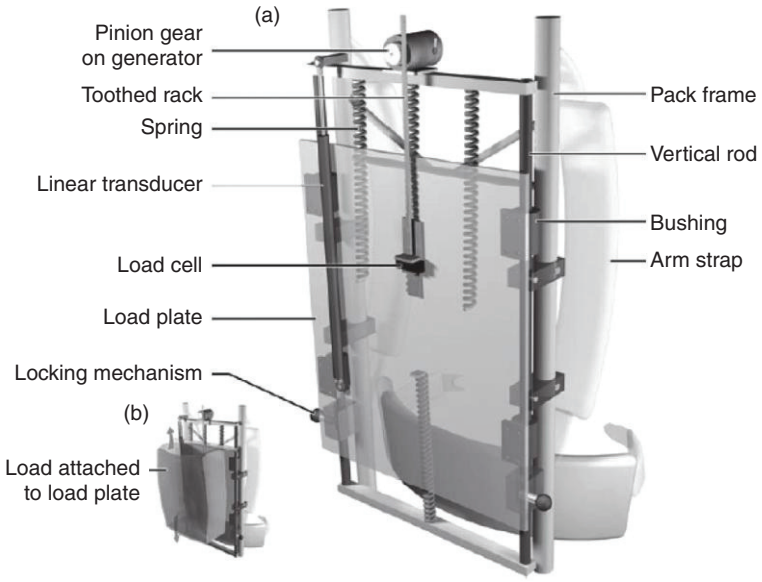

17.8 Backpack mounted motion harvesting device using PVDF by Granstrom *et al.*[22] (a) Device structure and (b) attachment of weight load. (Source: Copyright 2007, Institute of Physics Publishing.)

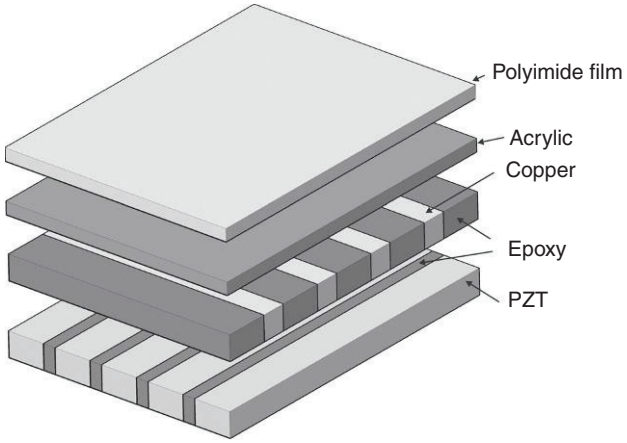

17.9 Typical structure of macro-fibre composites (MFCs). (Source: Adapted from Sodano *et al.*[8])

The main reason is that the particular interdigitated structure shown in Fig. 17.4 has been shown to be inefficient for current generation.[23]

Another approach for piezoelectric composites is to integrate a monolithic piezoelectric material into an elastic carrier. The resulting structure is far

© Woodhead Publishing Limited, 2012

less elastic than MFCs but it is more susceptible to strain than pure ceramics. This technique has been used in commercial piezoelectric sensors and actuators such as the Quick Pack implementation from Mide Technology Corporation, which is a bimorph device of a piezoelectric integrated into epoxy. A comparison of PZT, MFC and Quick Pack technologies for energy harvesting was given by Sodano *et al.*[23]

A relatively new category of harvesters uses piezoelectric nanowires. Typically, such devices employ an array of a large number of nanowires that are charged when bent, transducing relative motion to electricity. PZT nanowire devices have been shown to provide power densities substantially higher than those typically reported for cantilever devices,[25] although the volumes are very small. Equivalently large power densities are expected from ZnO nanowire devices, reaching 1 mW/cm^2, with very high energy transduction efficiency (30%).[26] Although this approach demonstrates the high prospects of nanotechnology in future electronics, a variety of challenges such as device mass production, packaging and reliability have proven difficult to address, shifting energy harvesting from nanowires to the long term.

For further study of piezoelectric materials and energy harvesting, one can refer to the reviews of Anton and Sodano,[27] Khaligh *et al.*[28] and Muralt *et al.*[29]

17.4 Electrostatic harvesting

In electrostatic harvesting, the electrostatic force between charged bodies is used to transduce kinetic energy into electrical. A pair of charged parallel plates is an instructive example. This configuration is shown in Fig. 17.10.[30] The system has a capacitance C and is charged with an initial charge Q. Due to the opposite charges on the two plates, there is an electrostatic force F_{es} which is given by the following equation:[31]

$$F_{T,\text{es}} = \frac{Q^2}{2 \cdot \varepsilon_0 \cdot \varepsilon_r \cdot A} \qquad [17.7]$$

where ε_0 is the vacuum permittivity and A is the area of the plates. If one of the plates is moved perpendicular to the plate surface so that the distance d between the plates is increased (Fig. 17.10a), F_{es} will produce work against the motion. This work will be transformed into electrical energy and stored in the capacitor. The same will occur if the motion is parallel to the surface of the plates. This can be understood by considering that the electric field will be rotated by this motion and that the electrostatic force is parallel to the field. The corresponding geometry is illustrated in Fig. 17.10b.

© Woodhead Publishing Limited, 2012

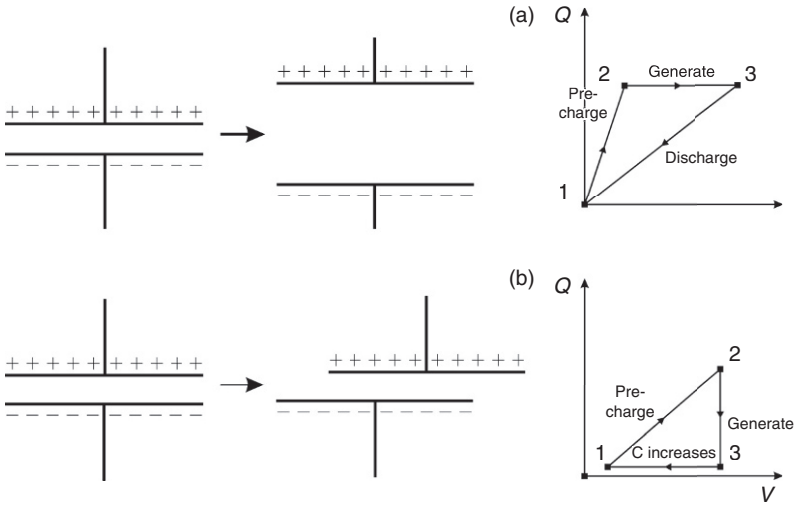

17.10 Electrostatic transduction with two charged parallel plates. (a) Displacement perpendicular to the plates, (b) displacement in parallel with the plates.[31]

Effectively, if the motion results in a change of capacitance, there will be conversion between mechanical and electrical energy, as long as there is some initial charge in the system. In order to provide the initial charge and exploit the incoming energy, a variety of system configurations exists. One of the most common is to keep a constant charge Q between the plates during motion. This can be done by charging the plates at a position of maximum capacitance C_{max} with a voltage V_{in}, supplying a charge $Q = C_{max} V_{in}$. Capacitance decrease to a minimum C_{min} will result in voltage increase to $V_{out} = Q/C_{min}$, and the charge Q can be discharged at a high voltage, hence supplying the harvested energy. This cycle of operation is illustrated in Fig. 17.10a. The harvested energy will be given by

$$\Delta E_{es} = \frac{1}{2} C_{min} V_{out}^2 - \frac{1}{2} C_{max} V_{in}^2 = \frac{1}{2} V_{in}^2 \frac{C_{max}}{C_{min}} \left(C_{max} - C_{min} \right) \qquad [17.8]$$

Another technique is to keep the voltage constant and let charge flow in or out of the plates during capacitance decrease or increase respectively. This technique is illustrated in Fig. 17.10b. For both cases, a general expression for the electrostatic force will be

$$F = -\frac{dE_{es}}{dz} = \frac{1}{2} \cdot \frac{Q^2}{C^2} \cdot \frac{dC}{dz} \qquad [17.9]$$

© Woodhead Publishing Limited, 2012

As quantitatively described by Equation [17.8], maximization of energy per cycle of operation requires a high priming voltage, high capacitance absolute values and a high capacitance ratio. At small scales, high capacitance values can be achieved by reducing the gap between the electrodes and by using high-k dielectrics. However, relative motion between the electrodes requires an air gap which dominates the dielectric space, and for this reason most electrostatic microgenerators use dielectrics as conventional as SiO_2. In other words, the critical factor for capacitance maximization is the air gap size rather than the dielectric permittivity.

However, for the priming of electrostatic generators, solid-state dielectrics are particularly important, as they can form electrets from which the required initial charging can be provided. Electrets are dielectrics with trapped charge that allows them to have (quasi) permanent polarization, much like the permanent magnetism of ferromagnetic materials. The lifetime of an electret's polarization can be hundreds of years.

A typical device orientation is shown in Fig. 17.11.[32,33] The electret is placed between the two capacitor plates. Its trapped charge creates an electric field which is equivalent to charging the capacitor with a high voltage (typically hundreds of volts). Any capacitance-changing relative motion of the plates, in-plane or perpendicular-to-plane, will result in charge motion through the wires, delivering electrical energy to a load resistance R. The electret provides the initial priming of the electrostatic harvesting device. Various geometrical implementations of such devices have been proposed including in-plane shifting electrodes,[32] rotating electrodes,[34] patterned electrodes[35] and comb-like electrode structures.[36] A quantitative analysis of the operation of such devices can be found in Tsutsumino *et al.*[35]

The fabrication of electrets typically involves deposition of a dielectric, implantation of charge and thermal annealing for charge stabilization. A variety of dielectric materials has been used for this purpose. A Plexiglas electret was the first to be used for electrostatic power generation in 1978, in a large scale (15 cm diameter) device for rotational motion.[37] In more recent

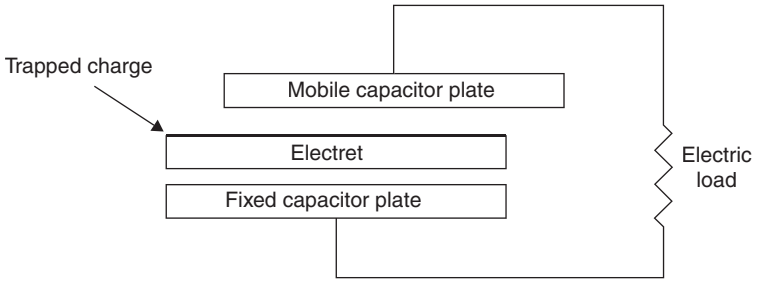

17.11 Operation principle of electret harvesting device for in-plane plate motion.

© Woodhead Publishing Limited, 2012

works and regarding specifically micro-generators, the main electret materials used are polytetrafluoroethylene (PTFE),[34,38,39] also known as Teflon, an amorphous perfluoropolymer called CYTOP,[33,40,41] Parylene[32] but also glass and ceramic dielectrics such as SiO_2 and Si_3N_4.[42–44]

The main technique for pre-charging the dielectrics is corona discharge.[40,41] The sample is placed near a high-voltage tip usually in the range of several kV. The high-potential gradient ionizes the air around the tip and, provided that there is no conducting path for arc discharge, a plasma is created. When exposed to this plasma, the dielectric acquires trapped charge. Alternative techniques involve ion implantation into the dielectric by conventional microelectronic implanters[42] or electron implantation by back-lighted thyratron devices.[38]

The critical characteristics of electrets are their surface charge density and corresponding voltage, lifetime and material/fabrication compatibility. Typical examples of electret materials with the charge density achieved by corona discharge are given in Table 17.1. The ceramic electrets appear to provide the largest charge densities, at the cost of high-temperature processing. PTFE and CYTOP are established polymer electrets with relatively low charge densities. Parylene is a promising, recently introduced material, although the reported charge stability lies in the range of one year, which needs to be improved. Ion implantation as an alternative to corona discharge has been shown to dramatically increase the charge density (16 mC/m^2) for SiO_2,[42] but again its lifetime adequacy requires further examination.

Various implementations of electrostatic energy harvesters have been reported in the literature, most employing electrets for the priming voltage. A comparison of electret-based harvesters can be found in Reference 45. Alternative methods for priming electrostatic generators have also been proposed. The use of intermediately stored electric power for priming through suitable circuitry is a viable option which, however, increases complexity and compromises the efficiency of the system. In addition, such approaches still require a method for device initialization. Another alternative method which was recently proposed is the direct use of a passive sensor with voltage output as the priming source of an electrostatic harvester. This approach is particularly relevant for wireless sensors and has

Table 17.1 Examples of common electret materials for electrostatic harvesting

Material	Charge density (mC/m^2)	Deposition technique	Charge implantation technique
PTFE[39]	0.54	Spinning	Corona discharge
CYTOP[33]	1.5	Spinning	Corona discharge
Parylene[32]	3.69	Room T – CVD	Corona discharge
SiO_2 /Si_3N_4[32]	11.5	AP-CVD	Corona discharge

© Woodhead Publishing Limited, 2012

led to implementations of simplicity and effectiveness.[46] The main challenge of this implementation is related to the voltage range of common passive sensors which is usually lower than that required for efficient operation of electrostatic harvesters.

17.5 Thermoelectric harvesting

In thermoelectric energy harvesting, the Seebeck effect is used to convert heat flow to electricity. The working principle is illustrated in Fig. 17.12. Two materials, A and B, are orientated such that one of their sides is kept at a low temperature $T1$ and the other at a high temperature $T2$. The materials are connected electrically at the hot side and the voltage across them is monitored at the cold side. The temperature difference will cause heat flow that is carried by free-moving particles such as electrons and holes, and by lattice vibrations – that is, phonons. In each material, the motion of charged particles will cause space charges at the contacts of both materials, which will in turn create an electric field opposing the motion, until equilibrium is reached. For two identical materials A = B, the resulting voltages will cancel out, but for different materials a non-zero total voltage V will appear. If a load is connected across the device output, a current will flow. Thereby, heat flow energy is converted to electrical energy. It is noted that the use of two materials is necessary, because the output terminals of the device must be at the same temperature. This structure is called a thermocouple.

The voltage V across a material with temperature difference ΔT can be written as $V = \alpha\Delta T$, where α is the Seebeck coefficient of the material. The relationship between V and ΔT is not linear and therefore α is temperature dependent. For the thermocouple in Fig. 17.12, $V = V_A - V_B = (\alpha_A - \alpha_B)\Delta T$.

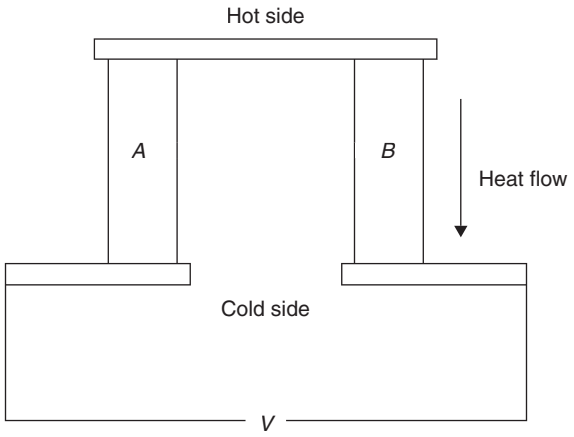

17.12 Working principle of a thermoelectric generator.

© Woodhead Publishing Limited, 2012

The parameter $\alpha = \alpha A - \alpha B$ is the Seebeck coefficient of the device. The output power of such devices is limited by the series resistance R of the thermocouple and also by the power conversion efficiency which is defined as the electrical output power W divided by the total heat flow Q. Therefore, the critical material properties for efficient thermoelectric generators are high Seebeck coefficient α, high electrical conductivity and low thermal conductivity K. The optimization of the last two properties can be challenging because decreasing the electronic component of thermal transport also means reduction of electrical conductivity. For this reason, materials with low phonon-driven thermal conduction are of special interest. A figure of merit typically used to compare thermoelectric generators in the literature is Z, defined as

$$Z = \frac{\alpha^2}{RK} \qquad [17.10]$$

where R is the series resistance of the thermocouple. Z is temperature dependent. The product of Z and average temperature T is used as another figure of merit, which is dimensionless and also temperature dependent. Given that the Seebeck coefficients of current devices and materials are in the range of hundreds of μV/K, the output voltage of thermal generators is another critical feature, which is usually addressed by connection of large numbers of thermocouples in series and use of long thermocouple structures. Finally, for energy-harvesting applications, scalability is added as another important material requirement. To summarize, thermoelectric energy-harvesting devices require a pair of materials with high electrical conductivity, low thermal conductivity, high Seebeck coefficient and scalable fabrication techniques.

Despite having substantially lower electrical conductivity than metals, semiconductors have been proven to be far more beneficial because of the high Seebeck coefficients of n-type/p-type material pairs. In addition they typically have lower thermal conductivities.

The most common semiconductor thermoelectric pair consists of a Bi_2Te_3–Sb_2Te_3 p-type alloy and a Bi_2Te_3–Sb_2Se_3 n-type alloy.[47–49] Fabrication involves deposition on a substrate and this can be efficiently achieved by thermal co-evaporation.[50] The corresponding generators have ZT values around 1. Examples of commercialization of these devices are the thermoelectric Seiko wrist watch[51] and the Micropelt generators.[47] Silicon has also been employed in p-type/n-type pairs,[52] which is a very promising structure because of its integrated circuit compatibility, accumulated material knowledge, processing know-how and scaling capability. Fabrication is also simple, involving mainly implantation of dopants. Poly-silicon and SiGe

© Woodhead Publishing Limited, 2012

have also been used in the same p-type/n-type orientation for thermoelectric generators,[53] allowing the formation of a very dense array of CMOS couples (59 400 in 6 mm^2) but with low aspect ratio and hence low efficiency. Finally, devices using n-polysilicon–aluminium thermoelectric pairs have been reported, showing potential for efficiency improvement.[54]

Along with those described earlier, a variety of alternative materials have been engineered for thermoelectric harvesting devices. n- and p-type superlattices of bismuth, antimony and selenium tellurides have been developed, demonstrating significant ZT improvement, to values greater than 3. This improvement is attributed to the additional phonon scattering within the superlattices, hence reducing the thermal conductivity while electrical conductivity remained relatively high.[55] Nanostructures of SiGe, Bi–Sb–Te have also been employed, achieving increased Seebeck coefficients due to increased Fermi-level density of states.[57] An indicative comparison of superlattice and conventional materials with respect to the ZT parameter has been performed by Venkatasubramanian *et al.*[57] and is shown in Fig. 17.13.

Nanotechnology has also been used for improving the performance of thermoelectric generators (TEGs). The use of Si[58] and Bi_2Te_3[59] nanowires has been investigated recently. In such thermoelectric devices, the nanowires which form the thermoelectric elements block large-wavelength phonon propagation due to their geometry, thereby reducing the thermal conductivity, while preserving the electrical conductivity. Promising results for nanoscale thermoelectric devices have also been predicted for graphene structures.[60] Quantum-well thermoelectric technology, employing

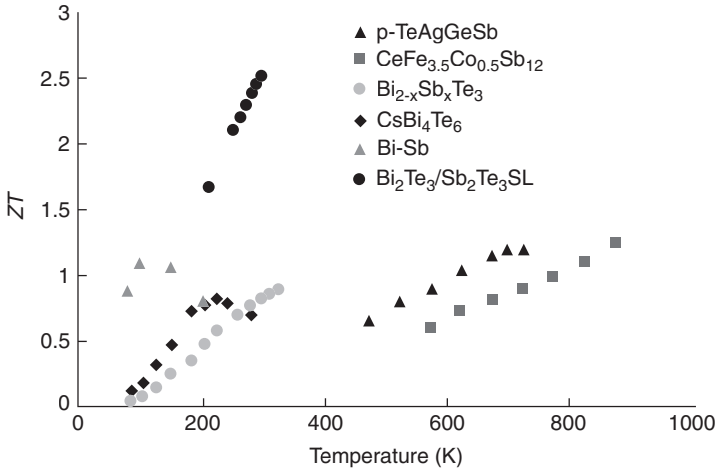

17.13 Comparison of superlattice materials with conventional semiconductor alloys. (Source: From Venkatasubramanian *et al.*[57] Copyright 2001, Nature Publishing Group.)

© Woodhead Publishing Limited, 2012

nanostructured multi-layer thin-films instead of Bi–Te materials, has been proposed and is used by the company Hi-Z, showing a fourfold efficiency increase.[61,62] These particular quantum well thermoelectrics consist of p-type/n-type Si/SiGe couples. Further techniques include thermoelectric junctions using ceramics. Candidate materials are ITO, ZnO and NiCrCoAlY/alumina nanocomposites. This type of thermal generator is particularly interesting for very high temperature gradients (over 500°C).[63]

The geometry of individual thermoelectric elements and their orientation in arrays is also very important for the performance of TEGs. A high aspect ratio is required to reduce thermal conductivity. Depending on the device orientation with respect to the substrate this is limited by the fabrication method. For a device using heat flow in parallel to the deposition direction, the device length is limited by the maximum deposition/implantation thickness. The maximum deposition thickness in scalable and parallel-fabrication micromachining is in the range of 100 μm. If the heat flow is perpendicular to the deposition direction, the device length can be orders of magnitude longer, resulting in higher transduction efficiency. An important challenge for this orientation is the prevention of parasitic heat flow through the substrate which compromises efficiency. In general, avoiding the distribution of the (already limited) temperature difference ΔT to device areas other than the thermocouple is another important aspect for efficient thermal generators.[64] To address this challenge, special structural designs employing CMOS compatible cavities and heat bridges have been developed[54,65] at the cost of device size and simplicity.

Pyroelectric energy harvesting uses temperature changes in time rather than space to produce electrical energy. The pyroelectric effect appears on dielectric materials with polar point symmetry, particularly where polarization is temperature dependent. Any temperature change will result in polarization change, which can appear as voltage across the dielectric. This effect is similar to the piezoelectric effect and therefore piezoelectric materials such as PZT and PVDF can also demonstrate pyroelectricity. These two materials have been recently studied for pyroelectric harvesting applications.[66] A maximum pyroelectric coefficient of 265 μC m^{-2} K^{-1} was found for PZT and 62 μC m^{-2} K^{-1} for PVDF. Other ceramic materials under investigation for pyroelectric harvesting include niobate/titanate compounds and lead magnesium niobate–lead titanate, PMN–PT. The piezoelectric properties of these materials have been discussed in Section 17.3. A review of their pyroelectric properties can be found in Sebald *et al.*[67] The theoretical efficiency of pyroelectric devices was studied as early as 1965 showing values in the range of a few per cent for a ΔT of 10 K using ferroelectrics such as potassium phosphates and niobates.[68] A characteristic feature of this type of harvesting is that it can take advantage of periodic temperature fluctuations, accumulating energy with every cycle.

© Woodhead Publishing Limited, 2012

An important limitation for the application of TEGs is the availability of temperature differences. Large ΔT values can be found in industrial and harsh environments, but in usual environmental conditions ΔT is restricted to a few degrees in the best case. This is a particular challenge for TEGs, as the efficiency of their operation increases with ΔT. In fact, for one thermoelectric couple at optimum operation, the efficiency will be given by the following equation:[69]

$$\eta_{\text{TEG}} = \eta_{\text{Carnot}} \cdot \frac{\sqrt{1+ZT}-1}{\sqrt{1+ZT}+\left(T_C/T_h\right)} \qquad [17.11]$$

where ZT is the product of the thermoelectric generator figure of merit Z defined in Equation [17.10] times the absolute temperature T. Assuming constant ZT efficiency is plotted against ΔT in Fig. 7.14. A cold-side temperature of $T_C = 300$ K is assumed. For ΔT values in the range of 20 K, a maximum efficiency of around 1% is expected.

A variety of applications for thermoelectric harvesting devices has been proposed. Waste thermal power recovery using thermoelectric generators has been proposed from power transistors[70] or automobile exhausts.[71] Telluride devices have been developed for electroencephalogram modules.[48] A generic wireless sensor platform including a telluride thermoelectric generator to recharge a solid-state battery has been developed by Micropelt and ST Microelectronics.[72] Quantum-well thermal generators for wireless sensors have been developed by Hi-Z technology Inc.[62]

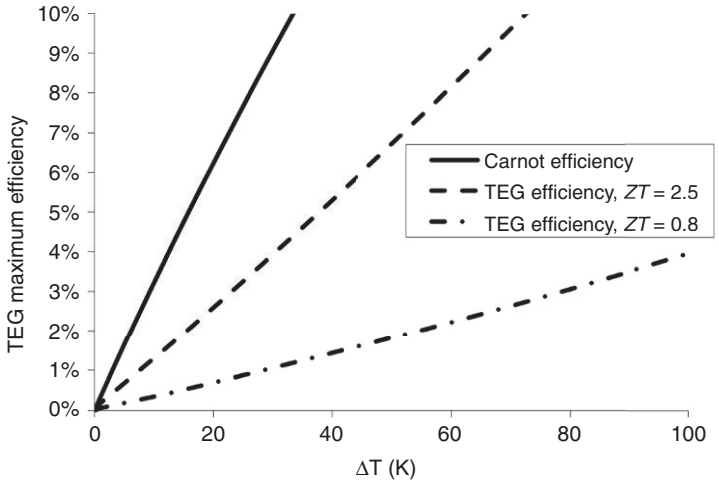

17.14 Maximum efficiency of TEGs calculated from Equation [17.11].

© Woodhead Publishing Limited, 2012

Finally, powering of wireless sensors for remote monitoring of aircraft seats by TEGs using the heat of the human body has been proposed.[73]

For most of the TEG applications mentioned previously, although ΔT is limited, the available heat is much greater than the capacity of the harvesters. The heat source can thus be considered as inexhaustible, providing a constant heat flow at a constant ΔT. Consequently, in such energy-harvesting cases, low efficiency doesn't necessarily mean poor device performance. Even a very small percentage of the available power may be enough for various energy-harvesting applications. However, there are application cases in which a limited amount of heat is available for exploitation. An example of such an application is the heat storage energy harvester recently proposed by Samson *et al*.[73,74] for avionic wireless networks. In such cases, the efficiency of the TEG is critical for successful operation and highly efficient thermocouple materials are highly desirable.

For further information regarding thermoelectric generators and energy-harvesting applications, see the literature review of Hudak *et al*.[55]

17.6 Electromagnetic energy harvesting from motion

In electromagnetic energy harvesting from motion, the traditional energy transduction mechanism of induction as described by Faraday's law is employed. Relative motion between a magnet and a coil results in magnetic flux variation which inducts an electromotive force across the coils. The motion is damped and the corresponding energy is transduced into electrical. At large scales, this is the dominant electrical power generation mechanism and is typically implemented for rotational motion. In energy harvesting however, the available motion comes more often in forms other than rotational, such as vibration or irregular forms such as the motion of the human body. For these reasons, various new electromagnetic generator architectures have been proposed for energy harvesting.

Electromagnetic motion energy-harvesting devices are traditionally classified into resonant, non-resonant and hybrid. This classification is illustrated in Fig. 17.15. Resonant devices are suitable mainly for vibration energy sources at a particular frequency, while non-resonant harvesters usually require rotational motion. Hybrid devices, such as the imbalanced rotor implementation of Fig. 17.15c, are designed to operate with a broader range of vibration frequencies or irregular motion. The main goal in this structural variation is to maximize the translation of the source motion into productive motion in the device. Optimization in this respect is very important, as it also is for the other two types of motion harvesters, namely piezoelectric and electrostatic. Another equally important goal which is specific to electromagnetic harvesting and common to all three categories of Fig. 17.15 is the maximization of magnetic flux through the coil structure. This depends on the strength,

© Woodhead Publishing Limited, 2012

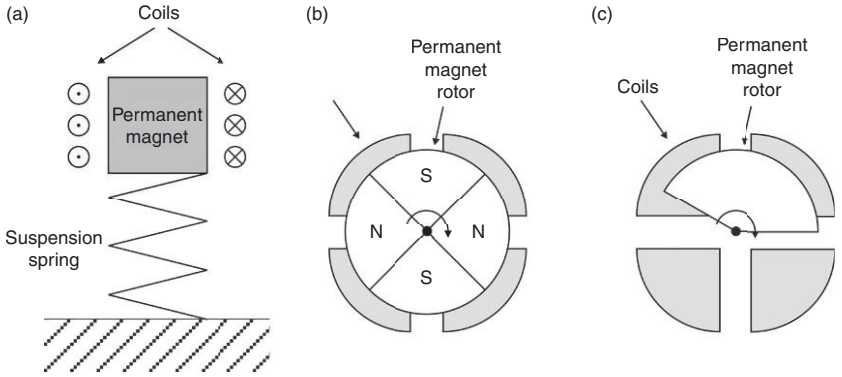

17.15 (a) Resonant, (b) non-resonant and (c) hybrid electromagnetic energy harvesting devices. (Source: Adapted from Khalig *et al.*[28])

orientation and location of the permanent magnet (PM) used and therefore, the physical and processing properties of the available PM materials are critical. The key desired properties of magnetic materials for electromagnetic harvesting are high residual magnetic flux density B_r, high coercivity H_c and potential for being placed and processed in the small scale.

The dominating hard magnetic material in the electromagnetic harvesting devices reported in the literature is neodymium iron boron (NdFeB). This material is the most popular commercialized rare-earth PM. It is been used in applications as common as hard disk drives. It has a residual magnetic flux density between 1 and 1.41 T, and coercivity between 760 and 1030 kA/m.[75] Samarium cobalt (SmCo) is another commercially available rare-earth magnet with residual magnetic flux density between 0.83 and 1.16 T, and coercivity between 600 and 840 kA/m.[75] While SmCo was the first to reach the market, NdFeB became dominant because of its higher strength and lower cost. SmCo is preferable for high-temperature applications, as its Curie temperature is around or over 1000 K, much higher than the Curie temperature of NdFeB (580 K).[75] Both NdFeB and SmCo are manufactured by sintering which involves heating a powder form of the material to temperature below the melting point. This restricts the ability for integration of the magnets with small-scale harvesters, and introduces limitations on the structural design.

Almost all electromagnetic motion harvesters reported in the literature use NdFeB as PMs, which have been commercially purchased and assembled in the device externally.[76–85] A performance comparison is presented in Table 17.2. Different structures have resulted in different performances, with the common limitation being the low flux density achieved at small scales. In larger scale devices, flux guidance is more efficient, taking advantage of the excellent rare-earth magnet properties. In most cases the PM has also been used as the proof mass, due to its large weight.

© Woodhead Publishing Limited, 2012

Table 17.2 Comparison of electromagnetic motion energy harvesters

Device	Institute	Year	Suspension material	Magnetic material	Freq. (Hz)	Acc. (m/s^2)	Proof Mass (g)	Vol. (cm^3)	Power (μW)
Beeby[81]	Southampton	2007	Silicon	NdFeB	52	0.589	0.66	0.15	46
PMG 7[81]	Perpetuum	2006	Steel	NdFeB	100	0.400	50	30	4000
Ching[85]	CUHK	2002	Copper	NdFeB	110	95.5	0.192	1	830
Shearwood[86]	Sheffield	1997	Polyimide	SmCo	4400	230	0.0024	0.025	0.3
El-Hami[79]	Southampton	2001	Steel	NdFeB	320	104	0.5	0.24	1000
Serre[87]	Barcelona	2007	Polyimide	NdFeB	360	1		0.6	0.2
PMG 17[88]	Perpetuum	2008			100	0.98		130	4500
VEH460[89]	Ferro Solutions	2009			60	1		170	5200
Kulah[90]	Michigan	2004	Parylene C	NdFeB	1			2.3	4
Pan[91]	Sun Yat Sen	2006	Silicon	FePt	60			0.45	100
Van Buren[92]	ETH	2007	Aluminium					30	35
Park[75]	Kwangwoon	2011	Silicon	NdFeB	53	4	0.046	0.6	102
Bouendeu[76]	IMTEK	2011	Polyimide	NdFeB	129	10	12.7	8	422
Yang[78]	NU Singapore	2010	None	NdFeB	50	19		2.7	0.4
Liao[82]	Chiao Tung	2009	Rotational	NdFeB	10krpm	–	–	0.2	7230
Duffy[84]	NU Ireland	2004	None	NdFeB	5		6	21	8500

© Woodhead Publishing Limited, 2012

In order to increase the power density of electromagnetic harvesters, new fabrication, integration and processing techniques for the previously mentioned materials are required. A variety of new techniques have been under development in recent years, towards the integration of rare-earth materials with micrometre-scale devices. For SnCo, sputtering of up to 50 μm thick films and patterning by use of ammonium cernitrate as an etchant has been reported.[86] Sputtered NdFeB films of thickness up to 8 μm and good magnetic properties have also been demonstrated.[87] Magnetron-sputtering of NdFeB on patterned Si and subsequent polishing has led to NdFeB patterns with thickness 12 μm.[88] Such structures are subsequently magnetized by application of a high magnetic field. The exploitation of these techniques is expected to lead to new types of electromagnetic energy harvesters in the near future.

Other magnetic materials with potential for integration with MEMS have also been proposed. Electrodeposited films of materials such as CoPt, CoPtP and FePt with thicknesses in the range of 1–10 μm have been reported.[89–92] Sputtered FePt layers have also been used for microgenerators.[93] A review of PMs for MEMS applications is given by Arnold and Wang.[94] Further information about various electromagnetic harvesting device implementations can be found in the literature reviews of Khaligh,[28] Arnold[95] and Mitcheson.[2]

17.7 Suspension materials for motion energy harvesting

One of the most critical goals of motion energy-harvesting devices is to achieve high performance from precisely the motion type that is available at a given application and location. While, for example, a variety of piezoelectric vibration energy harvesters of high performance have been developed, with energy per volume ratios over 0.1 mW/cm^3, their applicability is limited because they require operation at resonance and/or at a higher frequency than that of the available motion. In this respect, two main challenges emerge for motion energy harvesting: the development of low-resonance frequency oscillators at the small scale, and the development of inertial harvesting innovations with broadband operation.

For a single cantilever beam, the resonance frequency can be directly calculated from

$$f = \frac{1}{2\pi} \cdot \sqrt{\frac{k}{m}} \qquad k = \frac{E \cdot w \cdot \tau^3}{4 \cdot L^3} \qquad [17.12]$$

where E, w, τ and L are the Young's modulus, the width, the thickness and the length of a beam, respectively. The stiffness of the beam is k and a proof mass m is attached at the free end of the beam. Resonance frequency

© Woodhead Publishing Limited, 2012

calculations for a 10 mm long and 2 mm wide beam are shown in Fig. 17.16 for some common spring materials used in vibration energy harvesting. A proof mass of 0.1 g was assumed corresponding to the mass of a w-side cube of material with density 8000 kg/m^3. It is apparent that for low resonance frequency, beam thicknesses below 50 μm are required, even for elastic materials such as polyimide. For silicon, a beam thickness below 20 μm is required in order to achieve resonance below 10 Hz.

The effect of device scaling on resonance frequency is shown in Fig. 17.17, where a device with $w = L/5$, $\tau = L/200$ and $m = 8000$ kg/m^3 w^3 is assumed. Proportional scaling of all dimensions leads to increase of resonance frequency. Elastic materials such as polyimide reduce the resonance frequency by an order of magnitude, but the fabrication of single-beam resonators below 10 Hz at sizes smaller than 10 mm remains a challenge. The elastic modulus and tensile strength of the spring materials that are common in energy-harvesting devices are given in Table 17.3.

It is apparent that for MEMS device sizes (i.e., below 1 mm), new spring materials are desirable in order to achieve resonance frequencies below 10 Hz, particularly with Young's modulus values as low as 3– 4 orders of magnitude smaller than that of polyimide. Such materials should also be strong enough to support the corresponding proof mass under acceleration of 10–100 m/s^2, and compatible with scalable fabrication techniques. This combination of properties is difficult to obtain. As an unsuitable example, polydimethylsiloxane (PDMS) has an ideal Young's modulus but is viscoelastic (it behaves as a very viscous liquid), therefore it would be challenging to use in a solid-state device. On the other hand, beams made by silicon

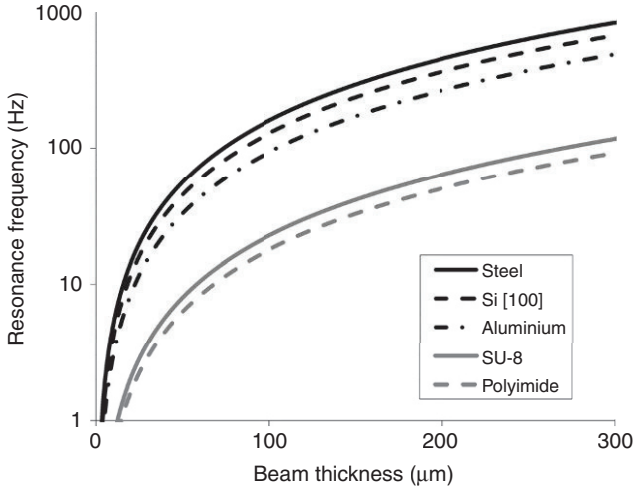

17.16 Beam resonance versus beam thickness calculations for a 10 mm long, 2 mm wide beam and a proof mass of 0.1 g.

© Woodhead Publishing Limited, 2012

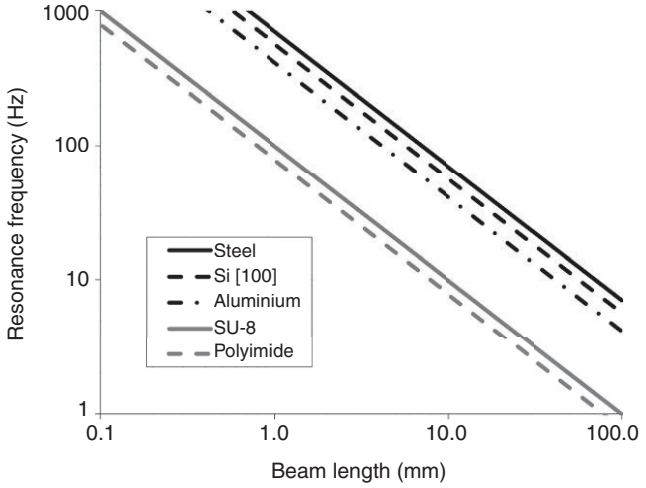

17.17 Beam resonance versus beam length calculations for a beam with length L, width $w = L/5$, thickness $\tau = L/200$ and proof mass $m = 8000\ \text{kg/m}^3\ \text{w}^3$.

Table 17.3 Elasticity properties of energy harvesting spring materials

Material	Young's Modulus	Tensile Strength	Reference
	GPa	MPa	
Aluminium alloys	69–73	90–570	102
Copper alloys	130	220–1310	
Stainless steel	193–204	415–1790	
Glass, borosilicate	70	69	
Silicon [111]	187		
Silicon [100]	130	130	
PMMA	2.24–3.24	48–72	
PET	2.76–4.14	48–72	
PTFE	0.40–0.55	21–34	
Polystyrene	2.28–3.28	36–52	
Polyimide	2.5	230	103
SU-8 Photoresist	4.02	34	
PDMS	0.36–0.87 E-3	2.24	
Parilene-C	3.2	70	104

nanowires exhibiting spring constants two orders of magnitude smaller than bulk silicon have been reported,[96] but further k reduction and integration challenges have yet to be addressed.

Due to these challenges, research and development on low-frequency mechanical oscillators for energy harvesting has focused on structural rather than material innovations. Typical simple adaptations of the beam structure include meander/spiral springs to extend the relative spring length[97] and

© Woodhead Publishing Limited, 2012

separate integration of rather large proof masses. New structures designed for mechanical frequency up-conversion have been introduced, on top of using low Young's modulus materials such as polyethylene terephthalate (PET) and styrene.[98,99]

Various novel ideas for broadening the optimized operation of motion energy harvesters have also been proposed. One of the simplest methods is to employ a detached proof mass concept, in which the mass can freely move by inertia inside a container. The elimination of springs results in non-resonant devices, at the cost of energy waste as the mass hits the boundaries. Such devices may be suitable for human motion and other stochastic motion source-related applications, such as body sensor networks.[100,101] Another approach is to use non-linear spring structures to broaden the efficient oscillation bandwidth of the proof mass. This can be done either indirectly by application of a secondary field that shifts the equilibrium suspension position of a spring structure,[102] or by using spring beams that form an angle with the motion axis, thereby exhibiting hardening or softening with increasing displacement.[103] Coupling multiple springs has also been shown to broaden the frequency range of operation of energy harvesters.[104] Finally, bi-stable non-linear structures have been proposed.[105]

17.8 References

1. N. S. Shenck and J. A. Paradiso, 'Energy scavenging with shoe-mounted piezoelectrics', *IEEE Micro,* vol. 21, pp. 30–42, 2001.
2. P. D. Mitcheson, E. M. Yeatman, G. K. Rao, A. S. Holmes, and T. C. Green, 'Energy harvesting from human and machine motion for wireless electronic devices', *Proceedings of the IEEE,* vol. 96, pp. 1457–1486, 2008.
3. E. Cross, 'Materials science: Lead-free at last', *Nature,* vol. 432, pp. 24–25, 2004.
4. Micromechatronics. (2011). *PZT materials data*. Available: http://www.mmech.com/pzt-materials-data
5. C. K. Mo, L. J. Radziemski, and W. W. Clark, 'Analysis of piezoelectric circular diaphragm energy harvesters for use in a pressure fluctuating system', *Smart Materials and Structures,* vol. 19, Article no 025016, pp. 1–10, 2010.
6. S. L. Kok, N. M. White, and N. R. Harris, 'Fabrication and characterization of free-standing thick-film piezoelectric cantilevers for energy harvesting', *Measurement Science and Technology,* vol. 20, Article no 124010, pp. 1–13, 2009.
7. K. Morimoto, I. Kanno, K. Wasa, and H. Kotera, 'High-efficiency piezoelectric energy harvesters of c-axis-oriented epitaxial PZT films transferred onto stainless steel cantilevers', *Sensors and Actuators A – Physical,* vol. 163, pp. 428–432, 2010.
8. H. A. Sodano, G. Park, and D. J. Inman, 'An investigation into the performance of macro-fiber composites for sensing and structural vibration applications', *Mechanical Systems and Signal Processing,* vol. 18, pp. 683–697, 2004.
9. D. N. Shen, J. H. Park, J. H. Noh, S. Y. Choe, S. H. Kim, H. C. Wikle, and D. J. Kim, 'Micromachined PZT cantilever based on SOI structure for low frequency

© Woodhead Publishing Limited, 2012

vibration energy harvesting', *Sensors and Actuators A – Physical,* vol. 154, pp. 103–108, 2009.
10. J. C. Park, J. Y. Park, and Y. P. Lee, 'Modeling and characterization of piezoelectric d(33)-mode MEMS energy harvester', *Journal of Microelectromechanical Systems,* vol. 19, pp. 1215–1222, 2010.
11. T. Harigai, H. Adachi, and E. Fujii, 'Vibration energy harvesting using highly (001)-oriented Pb(Zr, Ti)O-3 thin film', *Journal of Applied Physics,* vol. 107, Article no 096101, pp. 1–3, May 2010.
12. D. Koyama and K. Nakamura, 'Array configurations for higher power generation in piezoelectric energy harvesting', *Japanese Journal of Applied Physics,* vol. 49, pp. 1973–1976, 2010.
13. M. Renaud, K. Karakaya, T. Sterken, P. Fiorini, C. Van Hoof, and R. Puers, 'Fabrication, modelling and characterization of MEMS piezoelectric vibration harvesters', *Sensors and Actuators A – Physical,* vol. 145, pp. 380–386, 2008.
14. K. L. Ren, Y. M. Liu, X. C. Geng, H. F. Hofmann, and Q. M. M. Zhang, 'Single crystal PMN-PT/epoxy 1–3 composite for energy-harvesting application', *IEEE Transactions on Ultrasonics Ferroelectrics and Frequency Control,* vol. 53, pp. 631–638, 2006.
15. H. J. Song, Y. T. Choi, G. Wang, and N. M. Wereley, 'Energy harvesting utilizing single crystal PMN-PT material and application to a self-powered accelerometer', *Journal of Mechanical Design,* vol. 131, Article no 091008, pp. 1–8, 2009.
16. Z. G. Ye, B. Noheda, M. Dong, D. Cox, and G. Shirane, 'Monoclinic phase in the relaxor-based piezoelectric/ferroelectric Pb(Mg_{1/3}Nb_{2/3})O_{3}-PbTiO_{3} system', *Physical Review B,* vol. 64, p. 184114, 2001.
17. K. B. Kim, D. K. Hsu, B. Ahn, Y. G. Kim, and D. J. Barnard, 'Fabrication and comparison of PMN-PT single crystal, PZT and PZT-based 1–3 composite ultrasonic transducers for NDE applications', *Ultrasonics,* vol. 50, pp. 790–797, 2010.
18. 'Directive 2002/95/EC', *Official Journal of the European Union,* vol. 37, p. 19, 13.02.2003 2003.
19. Y. Saito, H. Takao, T. Tani, T. Nonoyama, K. Takatori, T. Homma, T. Nagaya, and M. Nakamura, 'Lead-free piezoceramics', *Nature,* vol. 432, pp. 84–87, 2004.
20. J. Tichý, J. Erhart, E. Kittinger, and J. Prìvratská, *Fundamentals of piezoelectric sensorics*. Springer, 2010.
21. V. Sencadas, S. Lanceros-Méndez, and J. F. Mano, 'Characterization of poled and non-poled -PVDF films using thermal analysis techniques', *Thermochimica Acta,* vol. 424, pp. 201–207, 2004.
22. J. Granstrom, J. Feenstra, H. A. Sodano, and K. Farinholt, 'Energy harvesting from a backpack instrumented with piezoelectric shoulder straps', *Smart Materials and Structures,* vol. 16, pp. 1810–1820, 2007.
23. H. A. Sodano, D. J. Inman, and G. Park, 'Comparison of piezoelectric energy harvesting devices for recharging batteries', *Journal of Intelligent Material Systems and Structures,* vol. 16, pp. 799–807, 2005.
24. Y. W. Yang, L. H. Tang, and H. Y. Li, 'Vibration energy harvesting using macrofiber composites', *Smart Materials and Structures,* vol. 18, Article no 115025, pp. 1–8, 2009.
25. B. Kumar and S. W. Kim, 'Recent advances in power generation through piezoelectric nanogenerators', *Journal of Materials Chemistry,* vol. 21, pp. 18946–18958, 2011.

© Woodhead Publishing Limited, 2012

26. Z. L. Wang and J. H. Song, 'Piezoelectric nanogenerators based on zinc oxide nanowire arrays', *Science,* vol. 312, pp. 242–246, 2006.
27. S. R. Anton and H. A. Sodano, 'A review of power harvesting using piezoelectric materials (2003–2006)', *Smart Materials and Structures,* vol. 16, pp. R1–R21, 2007.
28. A. Khaligh, P. Zeng, and C. Zheng, 'Kinetic energy harvesting using piezoelectric and electromagnetic technologies-state of the art', *IEEE Transactions on Industrial Electronics,* vol. 57, pp. 850–860, 2010.
29. P. Muralt, R. G. Polcawich, and S. Trolier-McKinstry, 'Piezoelectric thin films for sensors, actuators, and energy harvesting', *MRS Bulletin,* vol. 34, pp. 658–664, 2009.
30. P. D. Mitcheson, T. Sterken, M. E. Kiziroglou, E.M.Yeatman, and R. Puers, 'Electrostatic microgenerators', *Measurement and Control,* vol. 41, pp. 114–119, 2008.
31. Markus Zahn, *Electromagnetic Field Theory*: Massachusetts Institute of Technology: MIT OpenCourseWare. http://ocw.mit.edu (accessed October, 2011). License: Creative Commons Attribution-NonCommercial-Share Alike.
32. H. W. Lo and Y. C. Tai, 'Parylene-based electret power generators', *Journal of Micromechanics and Microengineering,* vol. 18, Article no 104006, pp. 1–8, 2008.
33. T. Tsutsumino, Y. Suzuki, N. Kasagi, and Y. Sakane, 'Seismic power generator using high-performance polymer electret', *MEMS 2006:19th IEEE International Conference on Micro Electro Mechanical Systems, Technical Digest,* pp. 98–101, 2006.
34. J. Boland, Y. H. Chao, Y. Suzuki, and Y. C. Tai, 'Micro electret power generator', *Mems-03: IEEE the Sixteenth Annual International Conference on Micro Electro Mechanical Systems,* pp. 538–541, 2003.
35. T. Tsutsumino, Y. Suzuki, and N. Kasagi, 'Electromechanical modeling of micro electret generator for energy harvesting', *Transducers '07 and Eurosensors XXI, Digest of Technical Papers, Vols 1 and 2,* pp. U436–U437, 2007.
36. T. Sterken, P. Fiorini, K. Baert, R. Puers, and G. Borghs, 'An electret-based electrostatic μ-generator', in *Transducers, Solid-State Sensors, Actuators and Microsystems, 12th International Conference on,* 2003, pp. 1291–1294, vol.2.
37. O. D. Jefimenko and D. K. Walker, 'Electrostatic Current Generator Having a Disk Electret as an Active Element', *Industry Applications, IEEE Transactions on,* vol. IA-14, pp. 537–540, 1978.
38. J. S. Boland, J. D. M. Messenger, K. W. Lo, and Y. C. Tai, 'Arrayed liquid rotor electret power generator systems', in *Micro Electro Mechanical Systems, 2005. MEMS 2005. 18th IEEE International Conference on*, 2005, pp. 618–621.
39. Y. Tada, 'Experimental characteristics of electret generator, using polymer film electrets', *Japanese Journal of Applied Physics,* vol. 31, p. 846, 1992.
40. D. Miki, M. Honzumi, Y. Suzuki, and N. Kasagi, 'Large-amplitude MEMS electret generator with nonlinear spring', in *Micro Electro Mechanical Systems (MEMS), 2010 IEEE 23rd International Conference on*, 2010, pp. 176–179.
41. T. Suzuki, S. Nagasawa, H. Okamoto, and H. Kuwano, 'Novel structure and fabrication of an energy harvesting device based on vibration-oriented generation for low oscillation operation', in *Sensors, 2009 IEEE*, 2009, pp. 1832–1835.
42. U. Mescheder *et al.,* 'Properties of SiO_2 electret films charged by ion implantation for MEMS-based energy harvesting systems', *Journal of Micromechanics and Microengineering,* vol. 19, p. 094003, 2009.

© Woodhead Publishing Limited, 2012

43. Y. Naruse *et al*., 'Electrostatic micro power generation from low-frequency vibration such as human motion', *Journal of Micromechanics and Microengineering,* vol. 19, p. 094002, 2009.
44. T. Sterken, P. Fiorini, G. Altena, C. Van Hoof, and R. Puers, 'Harvesting energy from vibrations by a micromachined electret generator', in *Solid-State Sensors, Actuators and Microsystems Conference, 2007. Transducers 2007. International*, 2007, pp. 129–132.
45. S. Boisseau *et al*., 'Optimization of an electret-based energy harvester', *Smart Materials and Structures,* vol. 19, p. 075015, 2010.
46. C. R. He, M. E. Kiziroglou, D. C. Yates, and E. M. Yeatman, 'MEMS energy harvester for wireless biosensors', *Mems 2010: 23rd IEEE International Conference on Micro Electro Mechanical Systems, Technical Digest,* pp. 172–175, 2010.
47. H. Bottner, 'Micropelt miniaturized thermoelectric devices: Small size, high cooling power densities, short response time', *ICT: 2005 24th International Conference on Thermoelectrics,* pp. 1–8, 2005.
48. J. P. Carmo, L. M. Goncalves, and J. H. Correia, 'Thermoelectric microconverter for energy harvesting systems', *IEEE Transactions on Industrial Electronics,* vol. 57, pp. 861–867, 2010.
49. L. M. Goncalves, P. Alpuim, and J. H. Correia, 'Fabrication of thermoelectric devices by applying microsystems technology', *Journal of Electronic Materials,* vol. 39, pp. 1516–1521, 2010.
50. J. P. Carmo, L. M. Goncalves, R. F. Wolffenbuttel, and J. H. Correia, 'A planar thermoelectric power generator for integration in wearable microsystems', *Sensors and Actuators A – Physical,* vol. 161, pp. 199–204, 2010.
51. M. Kishi, H. Nemoto, T. Hamao, M. Yamamoto, S. Sudou, M. Mandai, and S. Yamamoto, 'Micro thermoelectric modules and their application to wristwatches as an energy source', in *Thermoelectrics, 1999. Eighteenth International Conference on*, 1999, pp. 301–307.
52. D. M. Rowe, 'Thermoelectric generators as alternative sources of low-power', *Renewable Energy,* vol. 5, pp. 1470–1478, 1994.
53. M. Strasser, R. Aigner, M. Franosch, and G. Wachutka, 'Miniaturized thermoelectric generators based on poly-Si and poly-SiGe surface micromachining', *Sensors and Actuators A – Physical,* vol. 97–8, pp. 535–542, 2002.
54. T. Huesgen, P. Woias, and N. Kockmann, 'Design and fabrication of MEMS thermoelectric generators with high temperature efficiency', *Sensors and Actuators A – Physical,* vol. 145, pp. 423–429, 2008.
55. N. S. Hudak and G. G. Amatucci, 'Small-scale energy harvesting through thermoelectric, vibration, and radiofrequency power conversion', *Journal of Applied Physics,* vol. 103, Article no 101301, pp. 1–24, 2008.
56. M. S. Dresselhaus, G. Chen, Z. F. Ren, G. Dresselhaus, A. Henry, and J. P. Fleurial, 'New composite thermoelectric materials for energy harvesting applications', *JOM,* vol. 61, pp. 86–90, 2009.
57. R. Venkatasubramanian, E. Siivola, T. Colpitts, and B. O'Quinn, 'Thin-film thermoelectric devices with high room-temperature figures of merit', *Nature,* vol. 413, pp. 597–602, 2001.
58. E. Krali, C. Ki, K. Fobelets, and Z. A. Durrani, 'Seebeck coefficient in silicon nanowire arrays', presented at the *European Conference on Thermoelectrics*, Thessaloniki, Greece, 2011.
59. E. Koukharenko, X. Li, I. Nandhakumar, N. Frety, S. P. Beeby, D. Cox, M. J. Tudor, B. Schiedt, C. Trautmann, A. Bertsch, and N. M. White, 'Towards a

© Woodhead Publishing Limited, 2012

nanostructured thermoelectric generator using ion-track lithography', *Journal of Micromechanics and Microengineering,* vol. 18, Article no 104015, pp. 1–9, 2008.
60. D. Dragoman and M. Dragoman, 'Giant thermoelectric effect in graphene', *Applied Physics Letters,* vol. 91, Article no 203116, pp. 1–3, 2007.
61. S. Ghamaty, J. C. Bass, N. B. Elsner, 'Quantum well thermoelectric devices and applications', *22nd IEEE International Conference on Thermoelectrics, Proceedings ICT '03,* pp. 563–566, 2003.
62. V. Jovanovic, S. Ghamaty, N. B. Elsner, 'Design, fabrication and testing of quantum well thermoelectric generator', *2006 IEEE Proceedings 10th Intersociety Conference on Thermal and Thermomechanical Phenomena in Electronics Systems, Vols 1 and 2,* pp. 1417–1423, 2006.
63. O. J. Gregory, E. Busch, G. C. Fralick, and X. M. Chen, 'Preparation and characterization of ceramic thin film thermocouples', *Thin Solid Films,* vol. 518, pp. 6093–6098, 2010.
64. J. Bierschenk and IEEE, 'Optimized thermoelectrics for energy harvesting applications', *2008 17th IEEE International Symposium on the Applications of Ferroelectrics,* pp. 151–154, 2008.
65. S. M. Yang, T. Lee, and C. A. Jeng, 'Development of a thermoelectric energy harvester with thermal isolation cavity by standard CMOS process', *Sensors and Actuators A – Physical,* vol. 153, pp. 244–250, 2009.
66. A. Cuadras, M. Gasulla, and V. Ferrari, 'Thermal energy harvesting through pyroelectricity', *Sensors and Actuators A – Physical,* vol. 158, pp. 132–139, 2010.
67. G. Sebald, D. Guyomar, and A. Agbossou, 'On thermoelectric and pyroelectric energy harvesting', *Smart Materials and Structures,* vol. 18, Article no 125006, pp. 1–8, 2009.
68. E. Fatuzo, H. Kiess, and R. Nitsche, 'Theoretical efficiency of pyroelectric power converters', *Journal of Applied Physics,* vol. 37, pp. 510–516, 1966.
69. D. M. Rowe, *CRC Handbook of Thermoelectrics*. CRC Press, 1995.
70. K. J. Kim, F. Cottone, S. Goyal, and J. Punch, 'Energy scavenging for energy efficiency in networks and applications', *Bell Labs Technical Journal,* vol. 15, pp. 7–29, 2010.
71. E. A. Ibrahim, J. P. Szybist, and J. E. Parks, 'Enhancement of automotive exhaust heat recovery by thermoelectric devices', *Proceedings of the Institution of Mechanical Engineers, Part D: Journal of Automobile Engineering,* vol. 224, pp. 1097–1111, 2010.
72. S. a. Micropelt. (2010). *STMicroelectronics and Micropelt Demonstrate 'Perpetual Energy' Thermoharvesting Power Supply*. Available: http://www.st.com/internet/com/press_releases/t3020.jsp
73. D. Samson, M. Kluge, T. Becker, and U. Schmid, 'Wireless sensor node powered by aircraft specific thermoelectric energy harvesting', *Sensors and Actuators A: Physical,* vol. 172, pp. 240–244, 2011.
74. M. E. Kiziroglou, D. Samson, T. Becker, S. W. Wright, and E. M. Yeatman, 'Optimization of heat flow for phase change thermoelectric harvesters', in *PowerMEMS*, Seoul, Korea, 2011.
75. M. M. P. Association, 'Standard specifications for permanent magnet materials', MMPA standard no 0100–00, Magnetic materials producers association.
76. J. C. Park and J. Y. Park, 'A bulk micromachined electromagnetic micro-power generator for an ambient vibration-energy-harvesting system', *Journal of the Korean Physical Society,* vol. 58, pp. 1468–1473, May 2011.

© Woodhead Publishing Limited, 2012

77. E. Bouendeu, A. Greiner, P. J. Smith, and J. G. Korvink, 'A low-cost electromagnetic generator for vibration energy harvesting', *IEEE Sensors Journal,* vol. 11, pp. 107–113, January 2011.
78. D. A. Wang and K. H. Chang, 'Electromagnetic energy harvesting from flow induced vibration', *Microelectronics Journal,* vol. 41, pp. 356–364, June 2010.
79. B. Yang and C. Lee, 'Non-resonant electromagnetic wideband energy harvesting mechanism for low frequency vibrations', *Microsystem Technologies,* vol. 16, pp. 961–966, June 2010.
80. M. El-hami, P. Glynne-Jones, N. M. White, M. Hill, S. Beeby, E. James, A. D. Brown, and J. N. Ross, 'Design and fabrication of a new vibration-based electromechanical power generator', *Sensors and Actuators A: Physical,* vol. 92, pp. 335–342, 2001.
81. C. R. Saha, T. O'Donnell, N. Wang, and R. McCloskey, 'Electromagnetic generator for harvesting energy from human motion', *Sensors and Actuators A – Physical,* vol. 147, pp. 248–253, 15 September 2008.
82. S. P. Beeby, R. N. Torah, M. J. Tudor, P. Glynne-Jones, T. O'Donnell, C. R. Saha, and S. Roy, 'A micro electromagnetic generator for vibration energy harvesting', *Journal of Micromechanics and Microengineering,* vol. 17, pp. 1257–1265, July 2007.
83. L.-D. Liao, P. C. P. Chao, J.-T. Chen, W.-D. Chen, W.-H. Hsu, C.-W. Chiu, and C.-T. Lin, 'A miniaturized electromagnetic generator with planar coils and its energy harvest circuit', *IEEE Transactions on Magnetics,* vol. 45, pp. 4621–4627, October 2009.
85. S. P. Beeby, M. J. Tudor, R. N. Torah, E. Koukharenko, S. Roberts, T. O'Donnell, and S. Roy, *Macro and micro scale electromagnetic kinetic energy harvesting generators*, DTIP Conference, Stresa Italy 26–28 April, 2006.
85. M. Duffy, D. Carroll, and IEEE, 'Electromagnetic generators for power harvesting', in *Pesc 04: 2004 IEEE 35th Annual Power Electronics Specialists Conference, Vols 1–6, Conference Proceedings*, ed, 2004, pp. 2075–2081.
86. T. Budde and H. H. Gatzen, 'Thin film SmCo magnets for use in electromagnetic microactuators', *Journal of Applied Physics,* vol. 99, Article no 08N304, pp. 1–3, April 2006.
87. A. Walther, C. Marcoux, B. Desloges, R. Grechishkin, D. Givord, and N. M. Dempsey, 'Micro-patterning of NdFeB and SmCo magnet films for integration into micro-electro-mechanical-systems', *Journal of Magnetism and Magnetic Materials,* vol. 321, pp. 590–594, March 2009.
88. Y. Jiang, T. Fujita, M. Uehara, K. Kanda, T. Toyonaga, K. Nakade, K. Higuchi, and K. Maenaka, 'fabrication and evaluation of NDFEB microstructures for electromagnetic energy harvesting devices', presented at the PowerMEMS, Washington DC, 2009.
89. F. M. F. Rhen, E. Backen, and J. M. D. Coey, 'Thick-film permanent magnets by membrane electrodeposition', *Journal of Applied Physics,* vol. 97, Article no 113908, pp. 1–4, June 2005.
90. I. Zana, G. Zangari, J.-W. Park, and M. G. Allen, 'Electrodeposited Co-Pt micron-size magnets with strong perpendicular magnetic anisotropy for MEMS applications', *Journal of Magnetism and Magnetic Materials,* vol. 272–276, pp. E1775–E1776, 2004.
91. L. Vieux-Rochaz *et al*., 'Electrodeposition of hard magnetic CoPtP material and integration into magnetic MEMS', *Journal of Micromechanics and Microengineering,* vol. 16, p. 219, 2006.

© Woodhead Publishing Limited, 2012

92. F. M. F. Rhen, G. Hinds, C. O'Reilly, and J. M. D. Coey, 'Electrodeposited FePt films', *IEEE Transactions on Magnetics,* vol. 39, pp. 2699–2701, September 2003.
93. C. T. Pan, Y. M. Hwang, H. L. Hu, and H. C. Liu, 'Fabrication and analysis of a magnetic self-power microgenerator', *Journal of Magnetism and Magnetic Materials,* vol. 304, pp. e394–e396, 2006.
94. D. P. Arnold and N. Wang, 'Permanent magnets for MEMS', *Journal of Microelectromechanical Systems,* vol. 18, pp. 1255–1266, December 2009.
95. D. P. Arnold, 'Review of microscale magnetic power generation', *Magnetics, IEEE Transactions on,* vol. 43, pp. 3940–3951, 2007.
96. Á. San Paulo, N. Arellano, J. A. Plaza, R. He, C. Carraro, R. Maboudian, R. T. Howe, J. Bokor, and P. Yang, 'Suspended mechanical structures based on elastic silicon nanowire arrays', *Nano Letters,* vol. 7, pp. 1100–1104, 2007.
97. N. N. H. Ching, H. Y. Wong, W. J. Li, P. H. W. Leong, and Z. Wen, 'A laser-micromachined multi-modal resonating power transducer for wireless sensing systems', *Sensors and Actuators A: Physical,* vol. 97–98, pp. 685–690, 2002.
98. S. Jung, 'Energy-harvesting device with mechanical frequency-up conversion mechanism for increased power efficiency and wideband operation', *Appl. Phys. Lett.,* vol. 96, p. 111906, 2010.
99. H. Kulah and K. Najafi, 'An electromagnetic micro power generator for low-frequency environmental vibrations', in *Micro Electro Mechanical Systems, 2004. 17th IEEE International Conference on. (MEMS)*, 2004, pp. 237–240.
100. C. He, M. Kiziroglou, D. Yates, and E. Yeatman, 'A MEMS self-powered sensor and RF transmission platform for WSN nodes', *Sensors Journal, IEEE,* vol. 11, pp. 3437–3445, 2011.
101. M. E. Kiziroglou, C. He, and E. M. Yeatman, 'Rolling rod electrostatic microgenerator', *Industrial Electronics, IEEE Transactions on,* vol. 56, pp. 1101–1108, 2009.
102. L. Ji-Tzuoh, L. Barclay, and A. Bruce, 'The magnetic coupling of a piezoelectric cantilever for enhanced energy harvesting efficiency', *Smart Materials and Structures,* vol. 19, p. 045012, 2010.
103. D. S. Nguyen *et al.*, 'Fabrication and characterization of a wideband MEMS energy harvester utilizing nonlinear springs', *Journal of Micromechanics and Microengineering,* vol. 20, p. 125009, 2010.
104. T. Petropoulos, E. M. Yeatman, and P. D. Mitcheson, 'MEMS coupled resonantors for power generation and sensing', in *MicroMechanics Europe*, Leuven, Belgium, 2004.
105. R. Ramlan, M. Brennan, B. Mace, and I. Kovacic, 'Potential benefits of a nonlinear stiffness in an energy harvesting device', *Nonlinear Dynamics,* vol. 59, pp. 545–558, 2010.

© Woodhead Publishing Limited, 2012